

Colloidal dispersions and phase transitions in charged colloids

B. V. R. Tata

Materials Science Division, Indira Gandhi Centre for Atomic Research, Kalpakkam 603 102, India

Sterically stabilized as well as charge-stabilized colloidal dispersions mimic most of the phases of condensed matter and serve as excellent model systems to study the cooperative behaviour at micrometer length scales in equilibrium and non-equilibrium conditions. Charged-stabilized suspensions have the advantage of exhibiting structural ordering at much lower volume fractions as compared to sterically stabilized suspensions and is mainly due to the strong electrostatic interaction between the particles. The easy tunability of the interparticle interaction makes these systems ideally suited for studies of ordering phenomenon and the phase transitions under ambient conditions. Apart from novel applications of their ordered structures, it is the richness of the phase behaviour that makes the colloidal systems interesting from a fundamental point of view. Under certain conditions charge-stabilized suspensions are found to become inhomogeneous or undergo macroscopic phase separation. The underlying phase transitions have been identified. The phase separation phenomena observed in bulk suspensions of like-charged particles as well as microscopic investigations under confined geometries have generated considerable interest in reexamining the interparticle interaction in suspension of like-charged particles. This article reviews the structural ordering and phase transitions brought about by parameters such as particle volume fraction, surface charge density, salt concentration and polydispersity. In addition, the recent investigations of a two-dimensional system of charged large size metal balls, which has commonness with the charged colloidal system, are also discussed.

THE advances that have taken place in synthesizing polymer latex particles of well-defined shape and size^{1,2}, have paved the way for physicists to use colloidal dispersions of these and study their cooperative behaviour under equilibrium and non-equilibrium conditions by tailoring the interparticle interactions. In order to prevent their flocculation and make these suspensions stable, the particles are either coated with a thin layer (\sim nm) of polymer (steric stabilization) or sufficient charge is created (charge stabilization) on the

surface of the particles. Sterically stabilized suspensions (e.g. aqueous suspension of polymethyl-methacrylate (PMMA) particles) serve as nearly hard sphere suspensions and have been used to study the fluid–solid transition and glass transition^{3–6}. Aqueous suspension of polystyrene particles or colloidal silica constitute best examples for a charge-stabilized suspension^{7,8}. These particles become negatively charged (\sim 500 charges on a 0.1 μ m size particle) leaving equal number of tiny counterions in the medium making the suspension overall electrically neutral. In addition to the macroions (colloidal particles) and counterions there could be additional ions either due to the added salt (electrolyte) or due to the dissolved ionic impurities. The small ions (counterions and salt ions) screen the dominant Coulomb repulsive interaction between the macroions, hence controlling their concentration helps in tuning the strength as well as range of the interparticle interaction $U(r)$. In addition, varying the volume fraction ϕ ($= n_p \pi d^3/6$, where n_p is the number density) of the colloidal particles and the charge Ze on the particle also helps to tune $U(r)$.

One of the most fascinating aspects of colloidal dispersions is the appearance of long-range order. For instance, in the case of deionized suspensions of charged particles the long-range order appears even in extremely dilute ($\phi < 0.001$) dispersions. These structures, commonly known as colloidal crystals, were reported to exhibit iridescence arising from the Bragg diffraction (Figure 1) of visible light. Since the average interparticle distance is of the order of wavelength of light, laser light scattering can be used to characterize the structural ordering. The strong electrostatic interaction between the particles arrests the Brownian motion of the particles and induces a crystalline order. Depending on the suspension volume fraction and salt concentration C_s , the colloidal particles can undergo disorder–order transitions from fluid state to highly crystalline state of either face-centered cubic (fcc) or body-centered cubic (bcc) symmetry^{7,9}. Similarly hard-sphere colloids also undergo crystallization, but at much higher values of ϕ (ref. 5).

In addition to the crystalline order, these dispersions exhibit ordering similar to those found in atomic liquids^{10,11}, gases¹⁰, and even glasses^{12–14}. These fea-

e-mail: tata@igcar.ernet.in



Figure 1. Laser Bragg diffraction from colloidal crystals of aqueous suspension of charged polystyrene particles of $d = 120$ nm and $n_p = 8.1 \times 10^{12} \text{ cm}^{-3}$. The Bragg spots from large size crystals and the diffraction ring from small size crystals can be seen in the photograph taken in a back-scattered geometry using a He-Ne laser.

tures and the striking closeness of the magnitudes of the molar elastic constants¹⁵, latent heat of melting¹⁶ and other thermodynamic parameters of colloidal crystals with those of atomic solids allow one to regard colloidal dispersions as the scaled-up macroscopic versions of atomic systems. For instance, a colloidal dispersion with a particle concentration of about 10^{13} cm^{-3} has elastic constants¹⁷ of the order of 10 dynes/cm^2 , whereas those in atomic solids with atomic density around 10^{22} cm^{-3} have a value around $10^{12} \text{ dynes/cm}^2$. As a result of small elastic constants, colloidal crystals are extremely fragile and serve as the best example for systems of *soft condensed matter*. Similarly, latent heat of melting of colloidal crystals, when expressed in units of ‘per mole’ is the same as that of atomic solids. The perfect scaling of the magnitudes of the physical properties with particle concentration suggests that the interparticle interaction energy in colloids must be of the same order as the interatomic interaction in atomic systems. This has led many scientists to regard these as model systems to simulate condensed matter. In addition to this fundamental importance, colloidal crystals have found many applications such as those in optical Bragg filters¹⁸, switching devices¹⁹, photonic band gap materials^{20,21} and templates for synthesis of novel materials^{22,23}.

The crystalline order of colloidal particles can be destroyed by application of very small stresses; crystallized suspensions are easily shear-melted by simply tumbling the container. Furthermore, re-crystallization of the shear-melted metastable colloidal fluid is sufficiently slow (several minutes to hours) to allow the

measurement of structure and dynamics during the crystallization process. Similarly fluid-like suspension can be concentrated (density quench) to form a dense long-lived amorphous, non-ergodic phase. By contrast, fluids of simple atomic systems (inert gases or alkali metals) cannot be compressed sufficiently to bypass crystallization. For example, small-angle laser-light scattering studies of nucleation, growth and ripening of colloidal crystals³, which occurs over a time scale of several seconds, have clearly shown the existence of two different growth regimes – early nucleation and growth and late coarsening or ripening³. Similarly, shear stresses, much in excess of the shear strength of colloidal crystals, could be applied in the laboratory²⁴. Thereby properties of exotic non-equilibrium phases have been investigated. It is not easy to accomplish this in atomic systems except under shock conditions.

The parameters, which influence structural ordering and drive the phase transitions, are both intrinsic as well as extrinsic in nature. These include particle volume fraction ϕ , surface charge density σ , polydispersities of size and charge, ionic impurities, laser optical fields, shear, electric and magnetic fields. This article reviews some of the recent results that have been obtained by varying the suspension parameters in the area of ordering and phase transitions in charged colloidal systems. Recent observations such as gas–solid coexistence in highly charged colloids²⁵, occurrence of a reentrant solid–liquid transition²⁶, existence of long-lived metastable colloidal crystals²⁷, vapour–liquid condensation^{28,29}, reentrant transition^{28,30}, and stable voids^{25,31} suggest the existence of long-range attraction between like-charged particles. These observations have aroused considerable theoretical interest to propose models which predicted a long-range attraction in the effective pair-potential of charged colloidal particles^{32–34}. Alternatively, models without an explicit attractive term in the effective pair-potential also have been proposed^{35,36}. Long-range attraction in the effective pair-interaction has been found in confined suspensions^{37,38} and also in a 2D system of millimeter-sized charged metal balls³⁹. These experimental and theoretical results are reviewed. The theoretical understanding of these experimental observations with and without a long-range attractive term in the effective pair-potential is discussed. The need for further theoretical and experimental studies on the interparticle interaction and on the phase behaviour of charged colloids is also highlighted.

Phase transitions in homogeneous suspensions

Monodisperse suspensions of nearly hard sphere colloids are always homogeneous in the sense that the measured average interparticle distance is same as R_0 , where $R_0 \propto n_p^{-1/3}$. In other words, particles dispersed in

the solvent occupy the entire volume of the suspension having a uniform distribution. Since the attractive interactions are absent in a monodisperse suspension of hard sphere particles, they do not exhibit gas–liquid transition except undergoing fluid–crystal transition^{3,5,7} upon increasing the volume fraction ϕ beyond 0.49. At much higher volume fraction ($\phi > 0.58$) a glass-like order analogous to the Bernal glass also has been reported^{3,5,7}. Hard sphere suspensions have been studied extensively for understanding the kinetics of crystallization³ and dynamics of glass transition^{4,6}. Note that the volume fraction is the only parameter that is tunable in hard sphere suspensions to study the fluid–solid transition. Whereas in charge-stabilized suspensions, in addition to ϕ , salt concentration as well as charge on the particle can also be varied and phase diagrams (Figure 2) containing liquid, bcc, fcc and glassy phases have been reported^{7,9,14}.

The occurrence of crystalline, liquid-like and glass-like structures in charged colloids, their melting/freezing have been explained using theoretical calculations^{7–9,40} as well as computer simulations^{41–43} based on the screened Coulomb repulsive pair-interaction given by Derjaguin–Landau–Verwey–Overbeek (DLVO) theory⁴⁴. The DLVO pair-potential has the form

$$U_{\text{DLVO}}(r) = U_{\text{scy}}(r) + U_{\text{A}}(r), \quad (1)$$

where size corrected Yukawa term $U_{\text{scy}}(r)$ for particles of radius a with an effective charge Ze and dispersed in medium of dielectric constant ϵ is given by

$$U_{\text{scy}}(r) = \frac{e^2}{\epsilon} \left[\frac{Ze^{\kappa a}}{1 + \kappa a} \right]^2 \frac{e^{-\kappa r}}{r}, \quad (2)$$

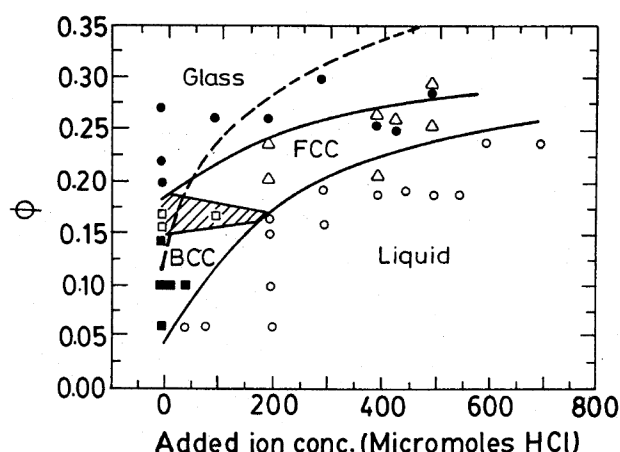


Figure 2. Experimental phase diagram of charged polystyrene colloidal suspension: \bullet , bcc; \circ , fcc; \blacksquare , liquid, and \blacktriangle , glass. The open squares in the hatched area mark the coexistence of bcc and fcc crystals. Taken from ref. 14 with the permission of the American Physical Society.

and the van der Waals attractive term is given by

$$U_{\text{A}}(r) = -\frac{A_{\text{H}}}{6} \left[\frac{2a^2}{r^2 - 4a^2} + \frac{2a^2}{r^2} + \ln \left(\frac{r^2 - 4a^2}{r^2} \right) \right], \quad (3)$$

where A_{H} is Hamaker constant and the inverse Debye screening length κ is given by

$$\kappa^2 = \frac{4\pi e^2}{\epsilon k_{\text{B}} T} (n_{\text{p}} Z + C_{\text{s}}). \quad (4)$$

The van der Waals attraction introduces a primary minimum⁴⁵ at very small interparticle separations and a secondary minimum at a distance of several times the particle diameter d in the pair-potential. Calculations show that the secondary minimum is ‘extremely shallow’ at low and moderate ionic strengths and the Coulomb barrier is sufficiently large to prevent the particles from experiencing the primary minimum. Hence, for all practical purposes, where ordering is observed at low ionic strengths the attractive part of the DLVO potential can be ignored.

Usually the effective charge and the residual salt concentration, which cannot be estimated precisely, are treated as the fitting parameters in calculations and making the comparison with experiments¹³. The total charge as well as the effective charge on the particle can be estimated experimentally from conductometric titration and conductivity experiments^{7,25} respectively (Figure 3). The actual charge is quite low as compared to the titratable charge because the degree of dissociation of the ionizable groups is always much less than unity. The charge estimated from conductivity experiments is often renormalized so that the calculated values can fit to the experimental ones.

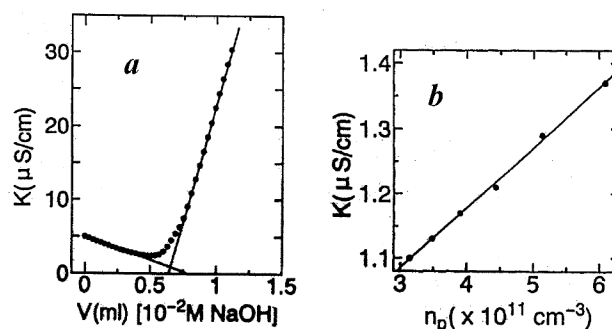


Figure 3. *a*, Conductivity of deionized aqueous suspension of poly(chlorostyrene-styrene sulfonate) particles of diameter 180 nm as function of added NaOH for measuring analytical charge density σ_{a} on the particles using the method of conductometric titration. σ_{a} ($= 7.0 \mu\text{C}/\text{cm}^2$) is estimated from the inflection point. *b*, Conductivity as function of particle number density n_{p} for suspension of same particles. Effective charge density σ ($= 0.25 \mu\text{C}/\text{cm}^2$) is estimated from the slope of the curve.

Deionized charged colloids exhibit fcc structure at large ϕ , which transforms to bcc as ϕ is reduced. The crystalline order melts into a liquid-like order either by decreasing ϕ or by increasing C_s . The applicability of Lindmann criterion for melting and the Hansen–Verlet criterion for freezing has also been tested for colloidal suspensions^{41–43}. In addition to these criteria, a simple dynamical criterion⁴⁶ for crystallization of a colloidal fluid has been proposed, which states that the ratio of the long-time and short time self-diffusion coefficient is 0.1 along the freezing line. This dynamical criterion is confirmed by probing the colloidal dynamics using forced Rayleigh scattering in dilute suspensions⁴⁶. The dynamics in concentrated suspensions, where multiple scattering is dominant, can be probed using diffusing wave spectroscopy (DWS)⁴⁷.

Effects of polydispersity

Size polydispersity (SPD) is inherent to colloidal suspensions and has considerable influence on ordering of hard sphere colloids. Since the surface charge on a particle is dictated by the size, SPD leads to charge polydispersity (CPD) and is important in the case of ordering of charged colloids. It is now possible to synthesize colloidal particles with desired diameter and desired surface charge density⁴⁸, hence one can in principle control the size as well as the charge on the particle rather independently and their polydispersities too. The SPD and CPD are best quantified in terms of the standard deviation of the size and charge with respect to their mean respectively, i.e.

$$\text{SPD} = (\langle d^2 \rangle - \langle d \rangle^2)^{1/2} / \langle d \rangle, \quad (5)$$

and

$$\text{CPD} = (\langle Z^2 \rangle - \langle Z \rangle^2)^{1/2} / \langle Z \rangle. \quad (6)$$

where $\langle d \rangle$ and $\langle Z \rangle$ represent the average diameter and average charge number respectively.

There have been several theoretical studies^{8,41–43} on the effects of SPD and CPD on structural ordering of hard sphere and charged-stabilized suspensions respectively. The crystallization in hard sphere colloids is suppressed for SPD values in the range of 6–11%. Recent experimental studies on the effect of particle size distribution on crystallization and glass transition showed interesting effects⁴⁹. The hard sphere suspension with a broad size distribution showed significantly lower crystallization rates as compared to the suspension with a narrow size distribution. In its colloidal glass state, no crystal growth was found to occur on secondary nuclei. These results are understood on the basis of long-time diffusion coefficients of the particles

and the large scale-diffusion required for accomplishing exchange of different sized particles.

In dilute charged colloids, where the average interparticle separation is several times the actual diameter of the particle CPD is expected to play dominant role than SPD. Whereas in concentrated suspensions both are important. The effect of CPD on the crystallization and melting of a charge polydisperse crystal has been investigated using Monte Carlo (MC) simulations^{8,41–43}. The crystalline suspensions are found to become amorphous beyond a critical CPD. By studying the behaviour of structural quantities, which are sensitive to the disorder, the CPD glass is found to be different from the atomic glass. Tata and Arora^{8,50} have examined in detail the possibilities of charge-ordered state at large values of CPD. The calculated Warren–Cowley short range order parameter⁵⁰, which characterizes the extent of charge ordering, suggested absence of any charge ordering. Further, systems evolved from widely different initial configurations and that from simulated annealing showed always a disordered state. From the studies of the stability of CPD glass and analysing the static disorder associated with the randomness in the pair-interactions, the disordered state of a CPD glass is stable equilibrium state⁵⁰. From the presence of static disorder (quenched-in randomness) and the frustration in packing of effective hard spheres associated with each charge, the CPD glass⁵⁰ is argued to be analogous to a spin-glass in atomic systems.

The phase diagram^{8,42,43} for a charge polydisperse colloidal suspension in the parameter space of CPD and C_s exhibits crystalline, amorphous and liquid-like ordered regions (Figure 4). Note that a charge polydisperse colloidal crystal at higher CPD needs lower values of C_s for melting. This is understood by defining the reduced temperature as $T^* = k_B T / U_0$, where U_0 is the nearest neighbour interaction energy. In a suspension with finite CPD, apart from the thermal fluctuations the frozen spatial disorder, arising due to the randomness in interparticle interactions, also contributes to weakening of structural correlations. Hence a charge-polydisperse system can melt even when the thermal contribution to randomness is smaller in magnitude, i.e. at lower T^* . The increase in the value of C_s or equivalently T^* at which charge polydisperse glass melts as a function of CPD is attributed to better stability of amorphous structure (against crystallization) away from crystal to amorphous phase boundary.

Phase transitions in inhomogeneous suspensions

Monodisperse hard sphere suspensions remain homogeneous except at the fluid–crystal transition and binary suspensions are found to exhibit phase separation⁵¹ due to the depletion attraction⁵². Whereas monodisperse

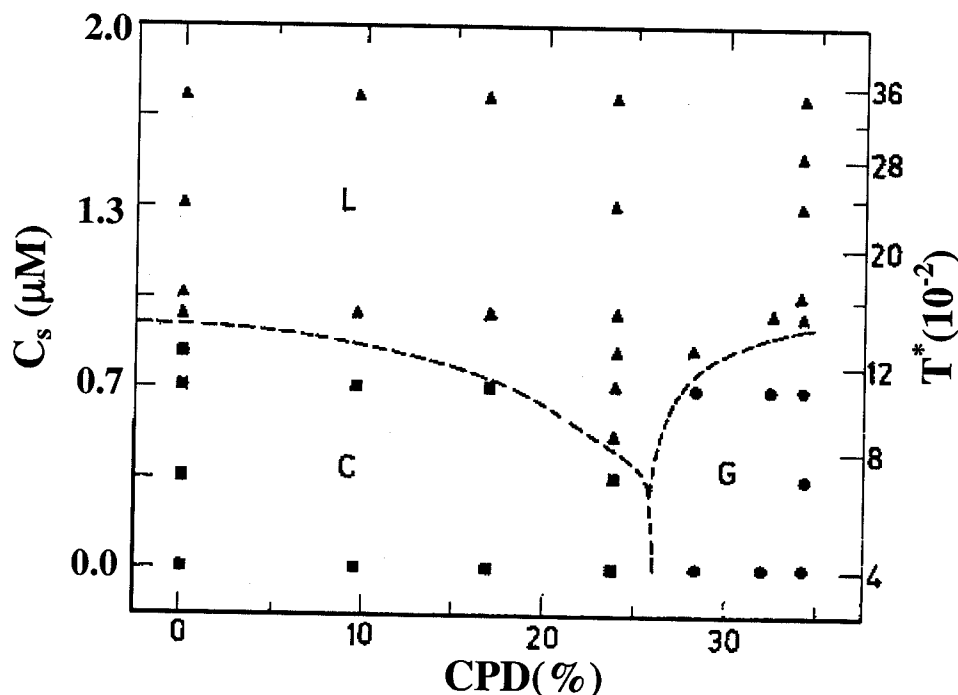


Figure 4. The phase diagram of charge polydisperse colloidal suspension with $n_p = 1.33 \times 10^{12} \text{ cm}^{-3}$. Δ , \square , and \circ represent the crystalline amorphous and liquid-like regions respectively. Broken curves representing phase boundaries are guides to the eye. The reduced temperature T^* corresponding to C_s is also marked on the y-axis. Taken from ref. 49 with the permission of the IOP Publishing Ltd. UK.

suspensions of charged colloids have been found to be in an inhomogeneous state in the form of gas–liquid^{8,10,28–30}, gas–solid coexistence^{8,25,53,54} and stable voids^{8,25,53,54} which suggested the existence of long-range attraction in the effective interaction contradicting the predictions of DLVO theory. These experimental observations are briefly discussed below.

Vapour–liquid condensation and reentrant transition

A phase separation analogous to vapour–liquid (VL) condensation in atomic systems has been reported in dilute colloidal suspension of polystyrene particles when either the impurity ion concentration is decreased or the volume fraction is increased^{8,10,28–30}. Deionized suspensions as function of ϕ exhibited VL condensation in the form of dense and rare phase below a critical volume fraction ($\phi_c < 1.12 \times 10^{-3}$)^{8,10,28,29}. Since the average interparticle separation at the volume fractions is of the order of wavelength of light, light scattering is the appropriate tool to study the structural ordering in these suspensions. Laser light scattering study of the structure factor $S(Q)$ in the phase separated state revealed the dense phase to be liquid-like ordered while the dilute phase to be gas or vapour-like^{10,28,29}. Suspensions were found to remain homogenous and liquid-like ordered above ϕ_c . In addition to this transition, the sus-

pensions also exhibited another phase transition during the deionization process^{8,10,28,30}. Suspensions which were initially homogenous (gas-like) underwent phase separation in the form of dense and rare phase region with C_s being lowered. Upon further reduction of C_s , suspensions whose concentration is above ϕ_c reentered into a homogeneous (liquid-like) state. Since the suspensions underwent phase separation only in a limited range of C_s and remained homogeneous on either side of this range, the transition was identified as a reentrant transition^{8,10,28,30}. There were some conjectures that the gradient in salt concentration was responsible for the occurrence of VL phase separation⁵⁵, which were subsequently shown to be incorrect⁵⁶.

Gas–solid transition

Apart from C_s and ϕ , the charge on the particle also influences strongly the strength and range of interaction and hence the structural ordering and phase behaviour of charged colloids. Suspensions with low effective charge showed VL condensation, whereas highly charged colloids have been predicted to show voids coexisting with ordered domains or disordered regions^{8,57,58}. Tata *et al.*^{8,25,53} have carried out experiments on aqueous suspensions of poly(chlorostyrene-sulfonate) particles having an effective charge

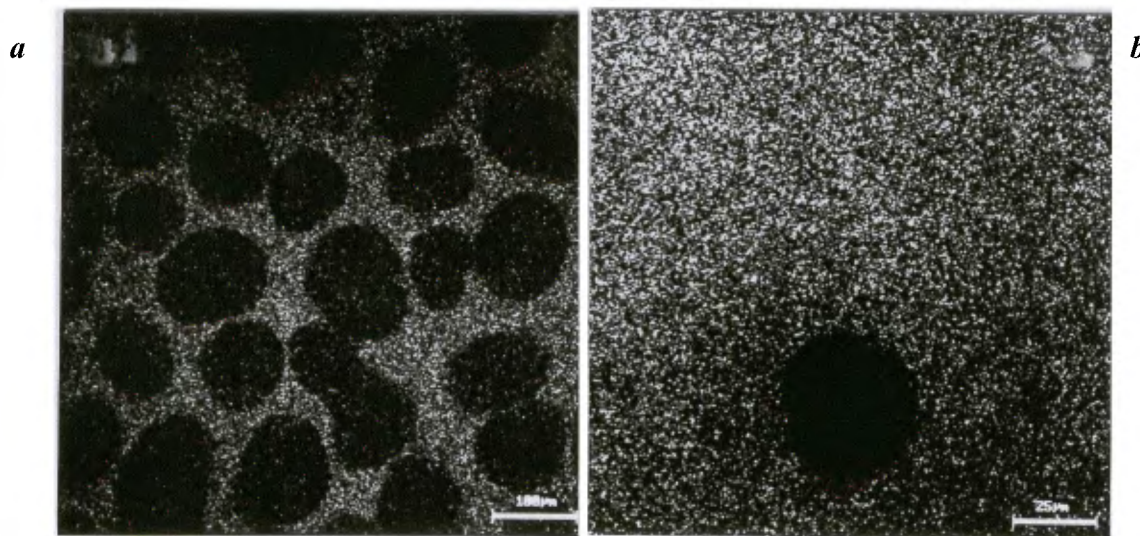


Figure 5. CLSM micrographs for aqueous suspension of poly(chlorostyrene-styrene sulfonate) particles with (a) $\phi = 0.006$ at a distance of 60 μm from the coverslip and (b) $\phi = 0.024$ at 46 μm .

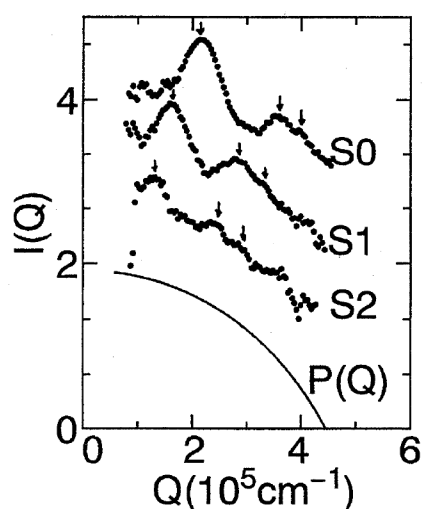


Figure 6. Desmeared USAXS intensity $I(Q)$ as a function of scattering wave vector Q for aqueous suspension of poly(chlorostyrene-styrene sulfonate) particles with $\phi = 0.06$ (S0), 0.024 (S1), and 0.012 (S2). Vertical arrows represent the positions of first and split second peak. Continuous line represents the theoretical particle structure factor $P(Q)$ for a spherical particle of 180 nm diameter. Taken from ref. 25 with the permission of the American Physical Society.

of 1590e. The ultra-small angle X-ray scattering (USAXS) and confocal laser scanning microscopy (CLSM) studies^{8,25,53} on these suspensions for ϕ in the range about 0.06–0.006 revealed coexistence of voids (Figure 5) with glass-like (Figure 6) disordered dense regions confirming the prediction. Observations on samples having $\phi < 0.006$ showed a macroscopic phase separation⁵³ with dense phase showing crystalline order being at the bottom of the sample cell and the rare

phase at the top with only a few particles. These investigations suggest occurrence of gas–solid transition⁵³ in deionized suspensions of highly charged particles.

Reentrant solid–liquid transition

Adding controlled amounts of $\text{K}_2\text{S}_2\text{O}_8$ during the synthesis can vary the charge on polystyrene particles^{1,7}. Whereas charge on silica particles can be tuned continuously by the addition of NaOH ⁴⁸. Recently, Yamana *et al.*²⁶ have investigated suspensions of colloidal silica and polystyrene particles using USAXS and CLSM techniques to study the influence of charge density σ ($=Ze/\pi d^2$) on solid–liquid phase transition. Suspensions having particles of low σ showed liquid-like order, which underwent crystallization upon increasing σ . Further increase in σ resulted in melting of the crystalline order into a liquid-like order, thus making reentrance. A phase diagram^{26,54} for the reentrant solid–liquid transition for colloidal silica is shown in Figure 7. The occurrence of a reentrant transition with increase in σ is unique to charged colloids and occurs at finite amount of salt concentration. These observations suggest that the highly charged colloids are unsuitable for making periodic structures which have found several applications^{18–23}.

Simulations and theoretical calculations

A purely repulsive pair-potential, predicted by DLVO theory, cannot explain the phase separation phenomena observed in inhomogeneous suspensions. This led Sogami and Ise (SI)³² to propose a theoretical formalism

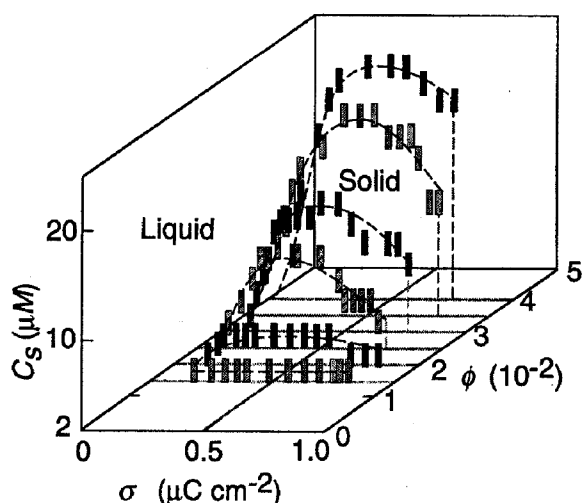


Figure 7. Phase diagram of aqueous dispersion of colloidal silica particle of diameter 120 nm showing reentrant solid-liquid transition as a function of effective charge density σ , volume fraction ϕ and salt concentration C_s . Rectangles represent the solid-liquid phase boundary. Dashed lines are guides to the eye. Taken from ref. 26 with the permission of the American Physical Society.

for charge-stabilized colloids which takes into account the presence of counterions and their interaction with macroions (colloidal particles). The effective Gibbs pair-potential $U_s(r)$ obtained from this model, has a long-range attractive term in addition to the usual repulsive screened Coulomb term and is given by

$$U_s(r) = \frac{Z^2 e^2}{\epsilon} \left[\frac{\sinh(\kappa a)}{\kappa a} \right]^2 \left(\frac{A}{r} - \frac{\kappa}{2} \right) \exp(-\kappa r), \quad (7)$$

where $A = 1 + (\kappa a) \coth(\kappa a)$. This pair-potential has minimum at R_m given by $R_m = [A + \{A(A+4)\}^{1/2}]/\kappa$ and depth $U_m = U_s(R_m)$. Note that R_m and U_m depend on κ which in turn depends strongly on suspension parameters, viz. ϕ , C_s , and Ze . The long-range attractive term in $U_s(r)$ arises due the mediation of counterions that are present in between the macroions (charged colloidal spheres).

Tata *et al.* have carried out MC simulations^{8,10,28,57-59} using $U_s(r)$ as function of ϕ , C_s , and σ . The simulations confirm the reentrant transition observed as function of decreasing C_s ^{10,28,59} and also the occurrence of VL condensation upon varying ϕ ^{8,58}. The occurrence of these transitions has been understood from the behaviour of R_m relative to the average interparticle spacing $R_0 = (\sqrt{3}/2)(2/n_p)^{1/3}$. The suspension is expected to phase separate when $R_m < R_0$, else it will remain homogeneous. The structural ordering in the dense phase depends on the magnitude of U_m . For $U_m \sim k_B T$ the dense phase is found to have a liquid-like order and for larger well depths a solid-like (crystalline or glass-like) ordering. The free energy calculations based on Barker

and Henderson perturbation theory showed a closed loop phase diagram⁶⁰ (Figure 8) containing gas-liquid coexistence and reentrant phase behaviour of dilute charged colloids. Simulations for low charge density particles using $U_s(r)$ also confirm the occurrence of a homogeneous fluid-phase at low volume fractions, which freezes into either bcc or fcc⁵⁸ upon increasing ϕ and lowering C_s . Suspensions remain in a homogeneous state because $R_m > R_0$ and the interaction at R_0 dictates the nature of ordering.

MC simulations as function of σ showed the occurrence of a homogeneous to inhomogeneous transition in deionized suspensions^{8,57}. At low σ , suspensions with low salt concentration are found to be homogeneous and crystalline. Beyond a critical σ , homogenous suspensions turn inhomogeneous in the form of voids coexisting with ordered or disordered (glass-like) regions. The charge density σ_c , at which the transition takes place depends strongly on the salt concentration in the suspensions^{8,58}. The experimental observation on deionized suspensions of highly-charged particles have confirmed formation of voids with glass-like disordered dense regions^{8,25}. The experimental observation of gas-solid transition is confirmed⁵³ by performing simulations for different values of ϕ . MC simulations as function of σ also predicted^{54,58} the occurrence of reentrant solid liquid transition which was confirmed experimentally^{26,54}. At low charge density, the well position $R_m > R_0$, hence the strength of interaction at R_0 determines the nature of ordering in these suspensions. When charge density of the particles is increased, the strength of interparticle interaction also goes up, resulting in a homogeneous crystalline order. Further increase in σ leads to decrease in well position and increase in well depths. When $R_m < R_0$ and $U_m \gg k_B T$, particles get trapped in large well depths leading to phase separation in the form of voids coexisting with ordered or disorder dense phase regions. At finite salt concentrations the voids collapse and the glass-like disordered regions also melt. As a result, the suspensions once again exhibit a liquid-like disorder. Thus the occurrence of reentrant solid-liquid transition observed with increase in σ is understandable. Ordered suspensions remaining inhomogeneous, and the effect of add salt on such inhomogeneous ordered structures⁶¹ can also be understood with proper renormalization of charge on the particles.

MC simulations using $U_s(r)$ could provide a satisfactory explanation for most of the experimental observations in charged colloids. However, the SI theory has not been accepted widely because the Gibbs pair-potential alone has the long-range attractive term but not in the Helmholtz pair-potential³⁶. Recently Schmitz⁶² reported a thermodynamic picture for the origin of attraction in the SI theory by focusing the attention on the electrical part of the Helmholtz and Gibbs-free energies and its dependence on the screening

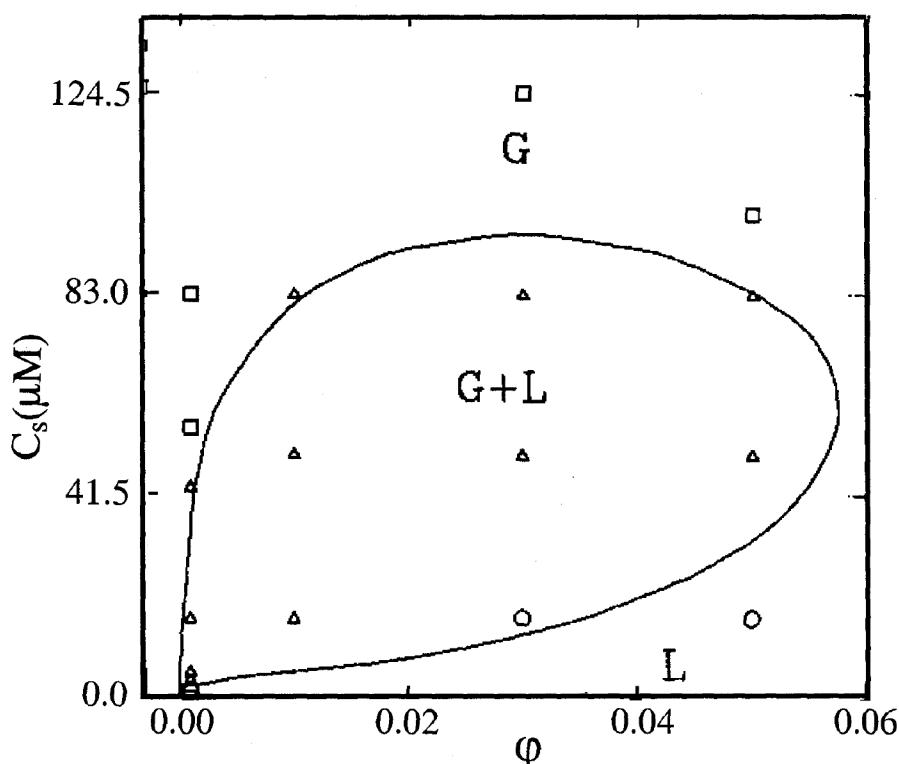


Figure 8. Gas-liquid phase diagram for an aqueous suspension 109 nm particles having an effective charge 500e. Symbols (□, △) represent gas (G), liquid (L) and its coexistence (G + L) respectively obtained from MC simulations and the closed curve is obtained from free energy calculations using Barker and Henderson model.

parameter κ . He showed that these electrical parts of the two free energies are not equal when κ is finite. This difference is attributed to the internal pressure due to confinement of the counterions to the vicinity of the macroions. There have been other attempts to obtain an effective interparticle interaction based on integral equation methods (IEM)³³ as well as obtaining solutions³⁴ of Langevin equation coupled with a diffusion equation. These calculations also predicted the existence of long-range attraction similar to SI theory, nevertheless they provide a potential of mean force rather than an effective pair-potential. The similarity between these calculations and the SI theory is that both consider the finite number of macroions. The SI theory explicitly relates the macroion charging process to the release of counterions, whereas the DLVO theory considers a pair of charged particles immersed in an infinite electrolyte without an explicit relationship to the macroion charge to the release of counterions.

Recent theoretical calculations based on density functional theory³⁵ (DFT) and Debye-Hückel (DH) theory³⁶ of highly asymmetric electrolytes have attempted to understand the above-mentioned experimental observation in inhomogeneous suspensions. These calculations also showed the occurrence of gas-liquid, gas-solid and reentrant transitions without an explicit long-range

attractive term in the effective pair-potential. But, the agreement with experimental observations is poor. However, the importance of these calculations is that the occurrence of gas-liquid and gas-solid transitions does not necessarily imply the existence of an attractive component in the effective pair interaction between like-charged colloidal particles. Since there exist two kinds of explanations for the same phenomena, which of the two explanations is true, needs further theoretical and experimental investigations in probing the effective interaction in charged colloids.

Measurements of effective pair-potential

Several attempts have been made to verify the existence of long-range attraction in the effective pair-interaction $U(r)$ between like charged colloidal spheres by making measurements on very dilute suspensions^{8,37,38,63,64}. Under dilute conditions the pair-correlation function $g(r)$ is related to $U(r)$ by

$$g(r) = \exp[-U(r)/k_B T]. \quad (8)$$

Hence, $U(r)$ can be extracted by measuring $g(r)$. Digital optical video microscopy³⁷ and optical tweezers tech-

niques^{38,63} have been used to measure the $g(r)$. In optical tweezers technique, randomly selected pair of particles are held at fixed separations. Repeatedly blinking the laser tweezers and tracking the motion of the particles after their release (by keeping off the optical traps) using digital video microscopy allows one to obtain $g(r)$. In the case of conventional digital video microscopy, several snapshots of particles positions are used for computing the $g(r)$. In making these measurements, the suspensions were always subjected to confinement between two parallel glass plates, which were negatively charged^{37,38}. Early measurements of $U(r)$ by Vondermassen *et al.*⁶³ and those by Crocker and Grier⁶⁴ showed only repulsion, and were fitted to the DLVO potential. Hence these authors concluded that the measured $U(r)$ is consistent with the DLVO theory. On the other hand, in a similar measurement, Kepler and Fraden³⁷ found attraction at large r which on analysis⁶⁵ with the effective charge as fitting a parameter was found to be consistent with $U_s(r)$. Subsequently, Crocker and Grier³⁸ also discovered the long-range attraction in $U(r)$ for the cell-gaps less than 7 μm , and a repulsive potential for larger gaps. They conjectured the attraction to be due to many-body effects arising from the geometrical confinement between the charged plates. Their main conclusion was that the measurements provide an unambiguous evidence for the absence of long-range attraction predicted by SI theory. This has been refuted⁶⁶ recently by Tata and Ise, pointing out the limitations in their experiments. It is worth pointing out that the pair-potential for confined charged colloids by solving the Poisson–Boltzmann equation do not show any evidence for attraction⁶⁷. Whereas introducing a nonlinear correction⁶⁸ to it seems to show evidence for attractive component. In the case of confined colloids, the charge on the glass plates can enhance the attraction by way of providing counterions dissociated from the glass plates in addition to those from the particles.

Charged metal ball system

Recently Tata *et al.*³⁹ have reported occurrence of gas–liquid transition and existence of long-range attraction in the effective pair-potential between like-charged metal balls in an electrostatically interacting two-dimensional (2D) system of millimeter sized metal balls. Unlike the colloidal system, this electrostatically stabilized system is free from ionic impurities and intervening dielectric fluid. The metal balls spread on polystyrene surface, when subjected to gentle shaking under low humidity conditions, acquire positive charge leaving the counter charges on the polystyrene surface. These metal balls are highly charged ($Ze \sim 10^9 e$). In these experiments the shaking at a constant frequency helps not only in charging the ball but also imparts

motion to the balls, enabling them to explore the configuration space. The friction between the ball and the surface sets the lower limit in the shaking frequency ν for moving the balls on the surface which determines the energy scale, viz. $\Gamma = m\omega^2 d^2/2$, where m is the mass of the metal ball and $\omega = 2\pi\nu$. Γ is analogous to the thermal energy in the atomic systems and is estimated to be 18.5 milliergs. Tuning the shaking frequency amounts to varying Γ and hence, changing the kinetic energy of the metal balls. The dominant interball interaction is Coulombic repulsion and is sufficiently large for the system to exhibit 2D ordering (Figure 9). This 2D system of like-charged metal balls is shown to exhibit gas–liquid condensation upon increasing the area fraction ρ of particles³⁹.

For charged colloidal system $U(r)$ has been obtained directly using eq. (8) under very dilute conditions. Likewise Tata *et al.* extracted $U(r)$ from $g(r)$ for metal balls at very low values of ρ with Γ as the energy scale. The $U(r)$ (Figure 10) thus obtained clearly showed the existence of attraction between like-charged metal balls at an interball distance of 5.4 mm with a depth of about 0.2Γ . The origin of this attraction in the metal ball system has been understood by performing *ab-initio* MC simulations³⁹ which takes into account different electrostatic interactions in the system. These *ab-initio* calculations predicted the existence of long-range attraction in the effective force, which is consistent with experimental observations. These simulations also bring out the importance of multipoles associated with the finite size of the charged balls in enhancing the long-range attraction mediated by countercharges. Theoretical calculations of Ben-Tal⁶⁹, which attempt to explain the origin of repulsion between oppositely-charged colloidal particles, also point out the importance of finite size effects.

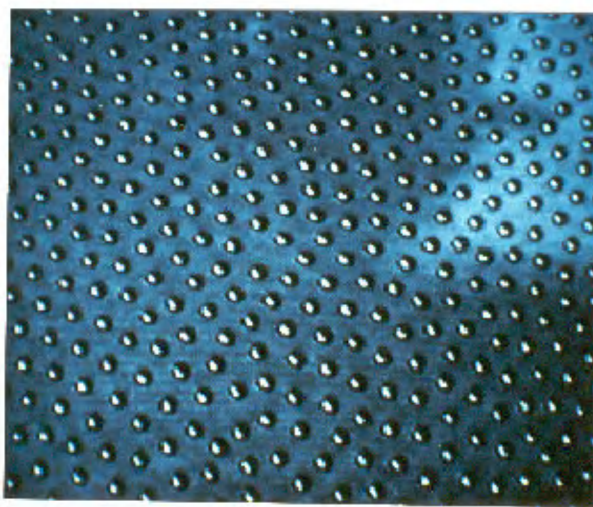


Figure 9. The photograph of charged metal balls of diameter 1.59 mm exhibiting 2D ordering at $\rho = 0.2$ on a polystyrene dielectric surface. Taken from ref. 39 with the permission of the American Physical Society.

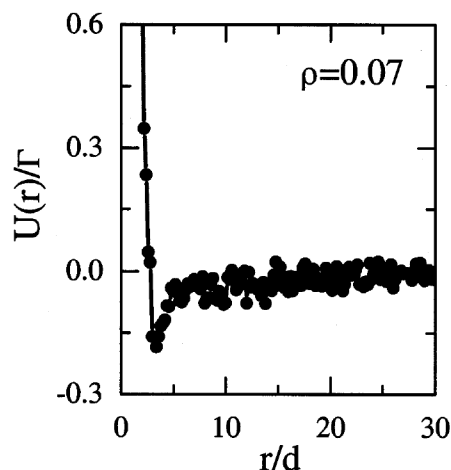


Figure 10. Pair-potential $U(r)$ (in units of $\Gamma = 18.5$ milliergs) between like-charged metal balls as function of interball distance r (in units of diameter of the ball = 1.59 mm) at $\rho = 0.07$. Taken from ref. 39 with the permission of the American Physical Society.

There exists a commonality between charged metal ball system and the charged colloidal system. Like colloidal particles, the metal balls are also charged. The counterions in the colloidal suspension are similar to the countercharges in the metal ball system. The colloidal particles span the configuration space by the Brownian motion, whereas metal balls change their configuration due to shaking. Though the energy and length scales differ widely in the two systems, what is common is the electrostatic interaction which is responsible for ordering of particles in both the systems. The long-range attraction in the effective pair-interaction of like-charged metal balls is observable because of the high charge density of the balls and absence of salt ions. Similar measurements on highly-charged colloids under extremely low salt concentrations are expected to show existence of long-range attraction. The report of long-lived pairs of like-charged colloidal particles by Yoshino⁷⁰ provides evidence for this.

Conclusions

Hard sphere suspensions as well as charge-stabilized colloidal systems offer enormous tunability in interparticle interaction to study the ordering and phase transitions at ambient conditions. The phase behaviour of hard-sphere colloidal systems is studied by varying the volume fraction. Hard sphere suspensions are considered as ideal systems to test the hard-sphere models which are exactly solvable. Studies of the crystallization kinetics and the glass transition in hard-sphere suspensions have revealed that nucleation requires large-scale particle diffusion, but crystal growth requires only small-scale particle motions. The volume fraction at which polydisperse suspensions undergo glass transition

is similar, irrespective of the size distribution of the particles. However, crystallization rates are found to be significantly slower in the case of polydisperse suspensions with broader distribution.

In charge-stabilized colloids, melting and freezing are studied by varying salt concentration and volume fraction, which are shown to be analogous to temperature and pressure in atomic systems. The charge on the particle is yet another important parameter which strongly influences the structural ordering as well as the nature of the suspensions. Deionized suspension of low charge density particles are homogeneous and their structural ordering can be understood equally well using DLVO potential or by $U_s(r)$. Suspensions of highly-charged particles or at high ionic strengths exhibit inhomogeneous nature in the form of gas–solid or gas–liquid coexistence and also the reentrant behaviour. Though simulations using $U_s(r)$ could provide satisfactory explanation for the observations in homogeneous as well as inhomogeneous suspensions, the recent calculations based on density functional and Debye–Hückel theory of asymmetric electrolytes have shown that these observations are understandable without a long-range attractive term in the effective pair-potential. Further, the measurements of effective pair-potential in dilute suspensions could not provide direct evidence for the existence of long-range attraction in the pair-potential due to the confinement by like-charged walls. Whereas the measurements on macroscopically large-size charged metal balls, which are free from charged wall confinement as well as ionic impurities, show evidence for existence of long-range attraction between like-charged metal balls. *Ab-initio* calculations to understand this attraction point out the importance of multipoles associated with finite size of the charged balls in enhancing the attraction mediated by countercharges. These multipoles are expected to be present even in charged colloids and need consideration in understanding the existence of long-range interaction between like-charged colloidal particles. Similarly, the experiments on dilute suspensions of highly charged colloids at very low salt concentrations, are expected to provide direct evidence and help in resolving the controversy on existence of long-range attraction. A good knowledge about the interparticle interactions is essential for better understanding of the phase behaviour of charge-stabilized colloids and making stable phases suitable for novel applications.

1. Ugelstad, J., Mork, P. C., Berge, A., Ellingsen, T. and Khan, A. A., in *Emulsion Polymerization* (ed. Piirma, I.), Academic Press, New York, 1982, ch. 11.
2. Chonde, Y. and Krieger, M., *J. Appl. Polym. Sci.*, 1981, **26**, 1819–1827.
3. Schätzel, K., in *Ordering and Phase Transitions in Charged Colloids* (eds Arora, A. K. and Tata, B. V. R.), VCH Publishers, New York, 1996, ch. 2.

4. van Megen, W., *Transport Theory Statist. Phys.*, 1995, **24**, 1017–1051.
5. Pusey, P. N. and van Megen, W., *Nature*, 1986, **320**, 340–342.
6. van Megen, W. and Underwood, S. M., *Phys. Rev. Lett.*, 1993, **70**, 2776–2779; *Phys. Rev.*, 1994, **E49**, 4206–4210.
7. Sood, A. K., in *Solid State Physics* (eds Eherenreich, H. and Turnbull, D.), Academic Press, New York, 1991, 45, p. 1.
8. Arora, A. K. and Tata, B. V. R., *Adv. Colloids Interface Sci.*, 1998, **78**, 49–97.
9. Chakraborti, J., Krishnamurthy, H. R., Sengupta, S. and Sood, A. K., *Ordering and Phase Transitions in Charged Colloids* (eds Arora, A. K. and Tata, B. V. R.), VCH Publishers, New York, 1996, ch. 9.
10. Tata, B. V. R., *Indian J. Pure Appl. Phys.*, 1994, **32**, 582–588.
11. Kesavamoorthy, R., Tata, B. V. R., Arora, A. K. and Sood, A. K., *Phys. Lett.*, 1989, **A138**, 208–212.
12. Kesavamoorthy, R., Sood, A. K., Tata, B. V. R. and Arora, A. K., *J. Phys. C: Solid State Phys.*, 1988, **21**, 4737–4748.
13. Lindsay, H. M. and Chaikin, P. M., *J. Chem. Phys.*, 1982, **76**, 3774–3781.
14. Sirota, E. B., Ou-Yang, H. D., Sinha, S. K., Chaikin, P. M., Axe, J. D. and Fujii, Y., *Phys. Rev. Lett.*, 1989, **62**, 1528–1531.
15. Crandall, R. S. and Williams, R., *Science*, 1977, **198**, 293–295.
16. Williams, R., Crandall, R. S. and Wojtowicz, P. J., *Phys. Rev. Lett.*, 1976, **37**, 348–351.
17. Kesavamoorthy, R. and Arora, A. K., *J. Phys. A: Math. Gen.*, 1985, **18**, 3389–3398.
18. Asher, S. A., Flough, P. L. and Washinger, G., *Spectroscopy*, 1986, **1**, 26–31.
19. Guisheng, Pan, Kesavamoorthy, R. and Asher, S. A., *Phys. Rev. Lett.*, 1999, **78**, 3860–3863.
20. van Blaaderen, A., Ruel, R. and Wiltzius, P., *Nature*, 1997, **385**, 321–325.
21. Sunkara, H. B., Jethmalani, J. M. and Ford, W. T., *Chem. Mater.*, 1994, **6**, 362–364.
22. Velev, O. D., Jede, T. A., Lobo, R. F. and Lenhoff, A. M., *Nature*, 1997, **389**, 447–449.
23. Wijnhoven, J. E. G. J. and Vos, W. L., *Science*, 1998, **281**, 802–804.
24. Ackerson, B. J., *Curr. Opin. Coll. Interface Sci.*, 1996, **1**, 450–453.
25. Tata, B. V. R., Yamahara, E., Rajamani, P. V. and Ise, N., *Phys. Rev. Lett.*, 1997, **78**, 2660–2664.
26. Yamanaka, J., Yoshida, H., Koga, T., Ise, N. and Hashimoto, T., *Phys. Rev. Lett.*, 1998, **80**, 5806–5809.
27. Larsen, A. E. and Grier, D. G., *Nature*, 1997, **385**, 230–233; *Phys. Rev. Lett.*, 1996, **76**, 3862–3865.
28. Tata, B. V. R. and Arora, A. K., *Ordering and Phase Transitions in Charged Colloids* (eds Arora, A. K. and Tata, B. V. R.), VCH Publishers, New York, 1996, ch. 6.
29. Tata, B. V. R., Rajalakshmi, M. and Arora, A. K., *Phys. Rev. Lett.*, 1992, **69**, 3778–3782.
30. Arora, A. K., Tata, B. V. R., Sood, A. K. and Kesavamoorthy, R., *Phys. Rev. Lett.*, 1988, **60**, 2438–2441.
31. Ito, K., Yoshida, H. and Ise, N., *Science*, 1994, **263**, 66–68.
32. Sogami, I. and Ise, N., *J. Chem. Phys.*, 1984, **81**, 6320–6332.
33. Chu, X. and Wasan, D. T., *J. Colloid Interface Sci.*, 1996, **184**, 268–278.
34. Tokuyama, M., *Phys. Rev.*, 1999, **E59**, R1–R4.
35. van Roij, R., Dijkstra, M. and Hansen, J. P., *Phys. Rev.*, 1999, **E59**, 2010–2025.
36. Warren, P. B., *J. Chem. Phys.*, 2000, **112**, 4683–4698.
37. Kepler, G. M. and Fraden, S., *Phys. Rev. Lett.*, 1994, **73**, 356–359.
38. Crocker, J. C. and Grier, D. G., *Phys. Rev. Lett.*, 1996, **77**, 1897–1900.
39. Tata, B. V. R., Rajamani, P. V., Chakrabarti, J., Nikolov, A. and Wasan, D. T., *Phys. Rev. Lett.*, 2000, **84**, 3626–3629.
40. Wang, G. F. and Lai, S. K., *Phys. Rev. Lett.*, 1999, **82**, 3645–3648.
41. Löwen, H., *Phys. Rep.*, 1994, **237**, 249–260.
42. Arora, A. K. and Tata, B. V. R., *Ordering and Phase Transitions in Charged Colloids* (eds Arora, A. K. and Tata, B. V. R.), VCH Publishers, New York, 1996, ch. 7.
43. Tata, B. V. R. and Arora, A. K., *J. Phys.: Condens. Matter*, 1991, **3**, 7983–7993; *ibid*, 1992, **4**, 7699–7708.
44. Verwey, E. J. W. and Overbeek, J. Th. G., *Theory of the Stability of Lyophobic Colloids*, Elsevier, Amsterdam, 1948.
45. Arora, A. K. and Rajagopalan, R., *Ordering and Phase Transitions in Charged Colloids* (eds Arora, A. K. and Tata, B. V. R.), VCH Publishers, New York, 1996, ch. 1.
46. Löwen, H., Palberg, T. and Simon, R., *Phys. Rev. Lett.*, 1993, **70**, 1557–1560.
47. Sanyal, S., Sood, A. K., Ramkumar, S., Ramaswamy, S. and Kumar, N., *Phys. Rev. Lett.*, 1994, **72**, 2963–2966.
48. Yamanaka, J., Koga, T., Ise, N. and Hashimoto, T., *Phys. Rev.*, 1996, **E53**, R4314.
49. Henderson, S. I., Mortensen, T. C., Underwood, S. M. and van Megen, W., *Physica A*, 1996, **233**, 102–116.
50. Tata, B. V. R. and Arora, A. K., *J. Phys.: Condens. Matter*, 1995, **7**, 3817–3834.
51. Dinsmore, A. D., Yodh, A. G. and Pine, D. J., *Phys. Rev.*, 1995, **E52**, 4045–4050.
52. Asakura, S. and Oosawa, F., *J. Polym. Sci.*, 1958, **33**, 183–188.
53. Tata, B. V. R. and Baldev Raj, *Bull. Mater. Sci.*, 1998, **21**, 263–278.
54. Ise, N., Konishi, T. and Tata, B. V. R., *Langmuir*, 1999, **15**, 4176–4184.
55. Palberg, T. and Würth, M., *Phys. Rev. Lett.*, 1994, **72**, 786.
56. Tata, B. V. R. and Arora, A. K., *Phys. Rev. Lett.*, 1994, **72**, 787.
57. Tata, B. V. R. and Ise, N., *Phys. Rev.*, 1996, **B54**, 6050–6053.
58. Tata, B. V. R. and Ise, N., *Phys. Rev.*, 1998, **E58**, 2237–2246.
59. Tata, B. V. R., Arora, A. K. and Valsakumar, M. C., *Phys. Rev.*, 1993, **E47**, 3404–3411.
60. Gupta, S. and Tata, B. V. R., *Solid State Phys. Symp. (India)*, 1994, **C37**, 389.
61. Matsuoka, H., Harada, T., Ikeda, T. and Yamaoka, H., *J. Appl. Cryst.*, 2000, **33**, 855–859.
62. Schmitz, K. S., *Langmuir*, 1996, **12**, 3828–3843.
63. Vondermassen, K. *et al.*, *Langmuir*, 1994, **10**, 1351–1353.
64. Crocker, J. C. and Grier, D. G., *Phys. Rev. Lett.*, 1994, **73**, 352–355.
65. Tata, B. V. R. and Arora, A. K., *Phys. Rev. Lett.*, 1995, **75**, 3200.
66. Tata, B. V. R. and Ise, N., *Phys. Rev.*, 2000, **E61**, 983–985.
67. Neu, J. C., *Phys. Rev. Lett.*, 1999, **82**, 1072–1074; Chan, D. Y. C., *J. Coll. Int. Sci.*, 1999, **213**, 268–269; Bowen, W. R. and Sharif, *Nature*, 1998, **393**, 663–664.
68. Goulding, D. and Hansen, J. P., *Euro. Phys. Lett.*, 1999, **46**, 407–410.
69. Ben-Tal, N., *J. Phys. Chem.*, 1995, **99**, 9642–9645.
70. Yoshino, S., *Polym. Int.*, 1993, **30**, 541–546.

ACKNOWLEDGEMENTS. I thank Dr A. K. Arora for fruitful collaboration and useful discussions.